THE JOURNAL OF BIOLOGICAL CHEMISTRY VOL. 286, NO. 46, pp. 39933–39944, November 18, 2011

Vascular Endothelial Growth Factor Receptor 2 Direct Interaction with Nephrin Links VEGF-A Signals to Actin in Kidney Podocytes*

Received for publication, March 23, 2011, and in revised form, September 14, 2011 Published, JBC Papers in Press, September 21, 2011, DOI 10.1074/jbc.M111.241620

Claudia Bertuccio[‡], Delma Veron[‡], Pardeep K. Aggarwal[‡], Lawrence Holzman[§], and Alda Tufro[‡1]

From the [‡]Department of Pediatrics, Yale University School of Medicine, New Haven, Connecticut 06520 and the [§]Division of Nephrology, University of Pennsylvania School of Medicine, Philadelphia, Pennsylvania 19104

Background: Excess VEGF-A down-regulates nephrin causing glomerular disease. Nephrin interacts with VEGFR2 *in vivo*.
Results: Nephrin-VEGFR2 interaction is direct, modulated by tyrosine phosphorylation, the VEGR2-nephrin complex involves Nck and actin, and VEGF-A signaling via this complex decreases cell size.
Conclusion: This interaction links extracellular VEGF-A to slit diaphragms and the podocyte actin cytoskeleton.
Significance: Our findings provide a molecular mechanism for VEGF-induced glomerular disease.

The transmembrane protein nephrin is an essential component of slit diaphragms, the specialized cell junctions that link podocyte foot processes. Podocytes are epithelial cells that surround the glomerular capillaries in the kidney and are necessary for the organ-filtering function. Nephrin signaling complex transduces extracellular cues to the podocyte cytoskeleton and regulates podocyte shape and function. Vascular endothelial growth factor A (VEGF-A) is a required growth factor produced and secreted by podocytes. Accumulating evidence suggests a cross-talk between VEGF-A and nephrin signaling pathways. We previously showed that *in vivo* nephrin associates with VEGF receptor-2 (VEGFR2), the signaling receptor for VEGF-A. In the present work, we characterized the interaction between nephrin and VEGFR2 in cultured cells and *in vitro*. We demonstrate that nephrin-VEGFR2 interaction is direct using mass spectrometry, immunoprecipitation, GST-binding assays, and blot overlay experiments. This interaction occurs through VEGFR2 and nephrin cytoplasmic domains. Nephrin-VEGFR2 interaction is modulated by tyrosine phosphorylation of both cytoplasmic domains. Furthermore, the nephrin-VEGFR2 complex involves Nck and actin. VEGF-A signaling via this complex results in decreased cell size. We provide evidence that this multiprotein interaction occurs in cultured podocytes. We propose that the nephrin-VEGFR2 complex acts as a key mediator to transduce local VEGF-A signals to the podocyte actin cytoskeleton, regulating the foot process structure and glomerular filter integrity.

Plasma ultrafiltration in the glomeruli is an essential kidney function. The glomerular filtration barrier consists of fenestrated endothelium, glomerular basement membrane, and slit diaphragms of the podocytes. Podocytes are specialized epithelial cells characterized by interdigitating foot processes linked by modified adherens junctions called slit diaphragms (1, 2). Slit diaphragms are composed of a backbone of nephrin molecules from adjacent foot processes that associate in cis and trans and form a zipper-like structure and interacting proteins, including FAT1, neph1, podocin. and P-cadherin (3–5).

Null mutations in the nephrin gene (NPHS1) cause congenital nephrotic syndrome of the Finnish type, a rare autosomal recessive disorder defined by massive albuminuria, hypoalbuminemia, dyslipidemia and edema (6). Kidney biopsies of infants with congenital nephrotic syndrome of the Finnish type reveal podocyte foot process effacement and absence of slit diaphragms (7). Nephrin is also down-regulated in acquired glomerular diseases associated with proteinuria and foot process effacement (8, 9). Phosphorylation of conserved tyrosine residues in the nephrin cytoplasmic domain (Tyr-1191, Tyr-1208, and Tyr-1232) by the Src kinase Fyn enables the binding and phosphorylation of cytoplasmic kinase PI3K and Nck adaptor proteins (10–14). Phosphorylated Nck interacts with neuronal Wiskott-Aldrich syndrome protein and stimulates the Arp2/3 complex, thereby regulating podocyte actin organization (15, 16). Podocyte-specific ablation of Nck2 in Nck1-deficient mice leads to massive proteinuria and lack of podocyte foot processes in newborn mice (17). Thus, nephrin provides permeability barrier for glomerular filtration, and contributes, via its intracellular signaling, to maintain the dynamic integrity of the podocyte architecture.

VEGF-A[2] is an essential growth factor produced and secreted by podocytes throughout life (18). Most VEGF-A signals are transduced by VEGFR2 (previously called Flk-1 in mice, and KDR in humans), a member of the receptor tyrosine kinase family (19). Homozygous deletion of VEGFR2 in mice is embryonic lethal, due to failure of vasculogenesis, whereas heterozygotes are normal (20). Binding of VEGF-A induces conformational changes in VEGFR2, dimerization, and autophosphorylation on tyrosine residues Tyr-1175, Tyr-1214, and others (21). Phosphorylated Tyr-1175 activates the MAPK

* This work was supported, in whole or in part, by National Institutes of Health Grant RO1-DK59333 (to A. T.).
[1] To whom correspondence should be addressed: 333 Cedar St., P.O. Box 208064, New Haven, CT 06520–8064. Fax: 203-785-3462; E-mail: alda.tufro@yale.edu.

[2] The abbreviations used are: VEGF-A, vascular endothelial growth factor A; VEGFR2, VEGF receptor-2; CD, cytoplasmic domain; $VEGF_{165}$, recombinant $rVEGF_{165}$; WB, Western blot.

pathway via phospholipase C γ (22) and is essential for vascular development during embryogenesis (23). Phosphorylation of VEGFR2 Tyr-1214 is required for the recruitment of Nck and Fyn and their phosphorylation, leading to actin polymerization, stress fiber formation, and endothelial cell migration (24).

We and others (25, 26) showed that VEGFR2 is expressed in podocytes *in vivo* by transmission electron microscopy, supporting previous reports demonstrating that VEGF-A signaling via VEGFR2 regulates podocyte survival and slit diaphragm interactions (27, 28). VEGF-A is increased in congenital nephrotic syndrome of the Finnish type and in acquired glomerular diseases associated with nephrin down-regulation, such as diabetic nephropathy (7, 29, 30). Our studies also showed that podocyte-specific $VEGF_{164}$ gain of function during development causes nephrotic syndrome in mice (31) and in adult mice, leads to proteinuria, podocyte effacement, and loss of slit diaphragms (25). Moreover, reversible VEGFR2 phosphorylation, down-regulation of nephrin, and co-immunoprecipitation of VEGFR2 and nephrin are associated with this phenotype, demonstrating a cross-talk between VEGF-A and nephrin signaling pathways *in vivo* (25).

The present study was designed to evaluate whether VEGFR2-nephrin interaction is direct using *in vitro* approaches. Our data demonstrate a direct interaction between the cytoplasmic domains of VEGFR2 and nephrin, which is modulated by phosphorylation. Moreover, we show that the VEGFR2-nephrin complex involves Nck and actin. We demonstrate that VEGF stimulation of this complex results in significant cell shape change in transfected cells, consistent with the foot process effacement phenotype observed previously *in vivo* (30, 31). We propose that the VEGFR2-nephrin complex transduces local VEGF-A signals to the podocyte actin cytoskeleton, thereby regulating cell shape and function.

EXPERIMENTAL PROCEDURES

Antibodies and Reagents—Antibody sources were purchased as follows: FLAG, Myc, α-actin (Sigma); GST, VEGFR2, and Nck (Santa Cruz Biotechnology); Nck (BD Transduction Laboratories); nephrin and HRP-conjugated anti-guinea pig (Fitzgerald Industries International); phosphotyrosine (Upstate Biotechnology); phospho-VEGFR2 (Tyr-1175) (Cell Signaling); and HRP anti-mouse and HRP anti-rabbit light chain (Jackson ImmunoResearch Laboratories). Rabbit polyclonal anti-nephrin and anti-phospho-nephrin antibodies were reported previously (13, 14). Heparin, recombinant mouse γ-interferon, anti-FLAG M2 affinity gel, and FLAG peptide were purchased from Sigma. Lipofectamine 2000, isopropylthio-b-D-galactoside, Cell Tracker®, and rhodamine phalloidin were obtained from Invitrogen. Protease inhibitor mixture and protein A-agarose beads were from Roche Diagnostics. Protein A/G-agarose was obtained from Pierce, and glutathione-Sepharose 4B beads were from GE Healthcare. pGEX4T-1 vector and ECL were from Amersham Biosciences, and BL21 and TBK1 *Escherichia coli* were from Stratagene. The mVEGF-A ELISA kit was from R&D Systems.

Eukaryotic Expression Constructs—Mammalian expression plasmids encoding mouse nephrin-Myc and FLAG-tagged Nck1 have been described previously (32, 33). Full-length mouse VEGFR2 cDNA was a gift of Dr. Lucia Pattarini (International Center for Genetic Engineering and Biotechnology). The cDNA-encoding mouse VEGFR2 open reading frame was subcloned into KpnI and ApaI sites of pcDNA 3.1. A FLAG epitope tag was placed at the 3′-end of the open reading frame using a standard PCR-based cloning technique. The FLAG-tagged mouse VEGFR2 cytoplasmic domain (VR2-CD) construct, corresponding to the last 561 amino acids of mouse VEGFR2 protein, as well as two fragments of it, VR2-162 encoding 162 amino acids (between 2353–2838 bp) and VR2-399 encoding the last 399 amino acids (between 2839–4035 bp), were generated by PCR from FLAG-tagged VEGFR2 and subcloned into pcDNA3.1. The VR2-CD, VR2-162, and VR2-399 were detected as ~75-kDa, ~18-kDa, and ~60-kDa proteins, respectively, when analyzed by SDS-PAGE under reducing conditions. Restriction digestion and DNA sequencing were used to validate all constructs.

Transient Transfection—COS-7 cells were transfected with mammalian expression plasmids (5–10 μg) using Lipofectamine 2000, following the manufacturer's instructions. Where indicated, cells were cultured in the presence of 50 μM pervanadate for 30 min prior to harvesting, or cells were serum-starved and incubated with heparin (50 units/ml) for 1 h, with or without recombinant $VEGF_{165}$ (50 ng/ml) for 30 min. Transfected cells were harvested with IP lysis buffer.

Generation of Podocyte Cell Line—Podocin-rtTA:*tet-O-VEGF* mice (25) were bred with *H-2Kb-tsA58* mice (34, Immortomouse®, The Jackson Laboratory, Bar Harbor, ME) to generate a conditionally immortalized podocyte cell line that overexpresses $VEGF_{164}$ in a doxycycline-regulated manner. Glomeruli were isolated from triple transgenic mice by standard serial sieving under sterile conditions (25, 34, 35), plated on collagen I-coated dishes, and cultured in RPMI 1640 medium (Invitrogen) with 10% FBS, 100 units/ml penicillin/streptomycin, and 100 units/ml recombinant mouse γ-interferon at 33 °C (permissive conditions). Following 5 days of primary culture, cells were trypsinized and passed through a 33-gauge needle to remove remaining glomerular cores. Cells were replated and propagated at 33 °C in medium containing 100 units/ml γ-interferon and subjected to dilution cloning. Clones were selected on the basis of their expression of podocyte-specific proteins (see Fig. 1*A*), morphology, and doxycycline-regulated $VEGF_{164}$ overexpression. Podocyte clones were propagated on collagen I-coated plates at 33 °C in RPMI 1640 supplemented with 10% FBS, 100 units/ml penicillin/streptomycin and in the presence of recombinant mouse γ-interferon (10 units/ml). Removal of γ-interferon and temperature switch to 37 °C inactivated the SV40 T antigen (see Fig. 1*C*) and induced podocytes to differentiate over ≥7 days.

Co-immunoprecipitation—Transiently transfected COS-7 cells or immortalized podocytes were lysed in IP lysis buffer containing 1% Triton X-100, 1% Nonidet P-40, 0.5% sodium deoxycholate, 150 mM NaCl, 10 mM Tris, pH 7.4, 1 mM EDTA, 50 mM NaF, and protease inhibitor mixture. After preclearing with protein A-agarose beads or with protein A/G-agarose, 0.5 mg of COS-7 cells or 1 mg of podocyte lysates were incubated with the appropriate antibody overnight at 4 °C under gentle rocking. Immune complexes were captured by adding protein

A-agarose or A/G-agarose beads for 4 h at 4 °C. After washing with IP lysis buffer, bound proteins were eluted in Laemmli buffer, and immunoprecipitated proteins were analyzed by Western blotting. Endogenous Nck was immunoprecipitated from 1.5-mg podocyte lysates by overnight incubation with anti-Nck at 4 °C. Immune complexes were incubated with protein A-agarose for 3 h, washed with IP lysis buffer, and eluted as above.

Immunoblot Analysis—Cell lysates (10 μg) or immunoprecipitates (10–40 μl) were resolved by 8% or 4–10% gradient SDS-PAGE under reducing conditions, transferred to nitrocellulose, incubated in blocking buffer (150 mM NaCl, 20 mM Tris, 5% (w/v) powdered milk, 0.1% Tween) and incubated with the following primary antibodies: rabbit anti-nephrin (1:1000) (34), or guinea-pig anti-nephrin (1:500), anti-VEGFR2 (1:300), anti-FLAG (1:2000), anti-GST (1:1000), anti-Nck (1:1000), anti-Myc (1:1000), anti-α-actin (1:5000), anti-phosphotyrosine (1:1000), anti-phospho-Tyr-1175 VEGFR2 (1:500), and anti-phospho-nephrin (1:1000) (36) antibodies. Subsequently, primary antibody binding was detected with HRP-conjugated anti-mouse (1:10,000), anti-rabbit (1:10,000 light chain), or anti-guinea pig (1:2000) secondary antibodies, as appropriate, and proteins were visualized with ECL. Densitometric analysis was performed using NIH ImageJ software.

Bacterial Fusion Protein Expression—Plasmids encoding a GST-CD-nephrin fusion protein, which includes the entire CD of mouse nephrin, and GST-CD-nephrin tyrosine (Tyr) residue point mutants (Y1191F, Y1208F, Y1191F/Y1208F, and Y1191F/Y1208F/Y1232F) were generated by PCR and cloned in frame into a pGEX4T-1 vector, as described previously (36). Fusion proteins were expressed in *Escherichia coli* BL21 and TKB1 at 37 °C and induced with 1 mM isopropylthio-β-D-galactoside. GST-tagged fusion proteins were purified using batch purification on glutathione-Sepharose 4B beads, following the manufacturer protocol.

GST-binding Assay—HEK cells were transfected with FLAG-tagged expression constructs. After 48 h, cells were washed and harvested in modified radioimmune precipitation assay buffer (50 mM Tris, pH 7.4, 200 mM NaCl, 1% Triton X-100, 0.25% deoxycholic acid, 1 mM EDTA, and 1 mM EGTA and protease inhibitors). Lysates were centrifuged, and the supernatant was incubated with anti-FLAG M2 affinity gel for 1 h under rotation at 4 °C. FLAG-tagged proteins were eluted from the resin by competition with FLAG peptide. Coomassie Blue staining and Western blot analysis confirmed the purity of FLAG-tagged proteins. Purified VEGFR2 FLAG-tagged proteins (1 μg) were incubated with 1 μg of purified GST-tagged fusion proteins in 500 μl of PBS for 2 h at 4 °C under rotation. The beads were collected by centrifugation and were washed five times with PBS. Bound proteins were eluted by boiling in Laemmli buffer, resolved by SDS-PAGE, transferred to nitrocellulose membranes, immunoblotted with anti-FLAG and anti-GST antibodies, and detected by ECL as described above.

Blot Overlay Assay—Purified GST-CD-nephrin (2–10 μg) and 10 μg of GST (control) was separated by SDS-PAGE and transferred to nitrocellulose membranes. After incubation with blocking buffer (5% (w/v) powdered milk, 0.1% Tween in PBS), membranes were probed with 0.3 μg/ml purified FLAG-tagged VEGFR2 in blocking buffer overnight at 4 °C. After extensive washing with blocking buffer, membranes were incubated with anti-FLAG antibody, followed by HRP-conjugated secondary antibody, and detected by ECL. As a positive control, 5 μg of lysate of COS-7 cells transfected with VEGFR2 was loaded in the same nitrocellulose membranes and immunoblotted with anti-FLAG antibody.

Mass Spectrometry Analysis—Lysates from COS-7 cells transfected with full-length VEGFR2 and nephrin constructs were subjected to immunoprecipitation with anti-nephrin antibody and resolved by SDS-PAGE. The gel was stained with Coomassie Blue, and bands at ~180 kDa were excised. These proteins were subject to *in situ* enzymatic digestion as described previously (37). The final peptide solutions were analyzed by LC-MS/MS (Thermo Scientific LTQ-Orbitrap XL mass spectrometer) at the W. M. Keck Foundation mass spectrometry facility at Yale University. Proteins were searched using Mascot Distiller and the Mascot search algorithm (38).

Immunocytochemistry—To examine the changes in cell morphology upon differentiation, podocytes were labeled live with Cell Tracker® following the manufacturer's instructions. Then, podocytes were fixed with 4% paraformaldehyde and incubated with rhodamine phalloidin. COS-7 cells transfected with VEGFR2, nephrin, or with both proteins were serum-starved and incubated with or without recombinant $VEGF_{165}$ (50 ng/ml) for 30 min, fixed, and stained with rhodamine phalloidin. Images were obtained using confocal microscopy (FV300, Olympus). COS-7 cell area was measured using NIH ImageJ software freehand area selection, on images obtained at ×120 magnification (×40 optics, ×3 digital) and expressed as mean ± S.E. μm^2 ($n = 15 + 2.4$ cells/experimental condition). For immunocytochemistry, differentiated mouse podocytes were grown on collagen I-coated glass coverslips, washed with PBS, and fixed with 4% paraformaldehyde for 10 min at room temperature, blocked with 2% donkey serum, 2% BSA, and 0.2% gelatin in PBS for 30 min, and incubated with anti-VEGFR2 and anti-nephrin antibodies overnight at 4 °C. Then, cells were incubated with Cy2 donkey anti-rabbit IgG and Cy3 donkey anti-guinea pig IgG, respectively. Nuclei were stained with Hoechst 33342 (Molecular Probes, Invitrogen). Cells were mounted with Vectashield (Vector Laboratories, Burlingame, CA) and examined by confocal microscopy.

ELISA—Podocyte VEGF-A was measured by ELISA in whole cell lysate and in conditioned medium from differentiated podocytes after 48 h induction with doxycycline (1 μg/ml) or vehicle and serum starvation for 8 h prior to analysis. Data were normalized for total protein concentration and expressed as % change from baseline.

Statistical Analysis—All experiments were performed at least three times. In ELISA experiments, readings from duplicate samples from three independent experiments were averaged, and data were expressed as mean ± S.E. Data were analyzed using unpaired *t* test or one-way analysis of variance as appropriate. Statistical significance was deemed as $p < 0.05$.

RESULTS

VEGFR2 and Nephrin Interact in Vitro and in Differentiated Podocytes—An inducible, immortalized mouse podocyte cell line was generated from *pod-rtTA*:*Vegf*$_{164}$ mice, harboring the

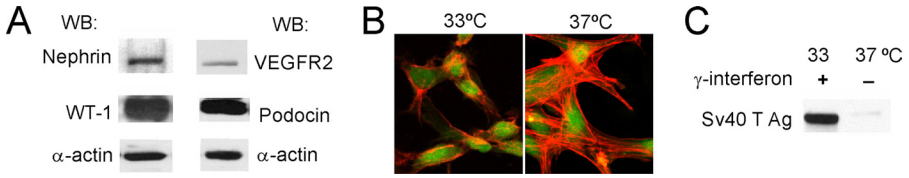

FIGURE 1. **Inducible mouse podocyte cell line expressing nephrin and VEGFR2.** *A*, Western blot (*WB*) of WT-1, nephrin, podocin, and VEGFR2 protein expression in differentiated murine podocytes cells. *B*, differentiated podocytes (37 °C) show typical cell shape, with extensive protrusions and F-actin filaments, as compared with undifferentiated podocytes (33 °C), Cell tracker® (*green*), rhodamin phalloidin (*red*). *C*, WB shows that SV40 large T antigen (*Ag*) is expressed only by undifferentiated podocytes (33 °C).

$Vegf_{164}$ transgene under a tetracycline-regulated promoter, using described methods (25, 42). This immortalized podocyte cell line expressed WT-1, nephrin, podocin, and VEGFR2 (Fig. 1*A*). Temperature switch from 33 to 37 °C induced podocyte differentiation, evidenced by cell morphology change and loss of SV40 expression (Fig. 1, *B* and *C*). Doxycycline induction of differentiated podocytes for 48 h resulted in a significant increase in cell-bound and secreted endogenous VEGF-A, detected by ELISA (67 ± 9.4% and 72 ± 20% above baseline, respectively, $p < 0.05$, $n = 4$).

To evaluate VEGFR2 interaction with nephrin, VEGFR2 was immunoprecipitated from cultured podocyte lysates, and the immunoprecipitates were probed by Western blot with the corresponding antibodies (Fig. 2*A*). Reciprocal co-immunoprecipitation experiments confirmed that endogenous VEGFR2 and nephrin associate in cultured podocytes. Immunocytochemistry showed that endogenous VEGFR2 and nephrin localized to the same compartments in cultured podocytes (Fig. 2*B*). This interaction was confirmed in COS-7 cells using an alternative approach. COS-7 cells were transiently co-transfected with Myc-tagged full-length nephrin and FLAG-tagged full-length VEGFR2 constructs. Nephrin and VEGFR2 co-immunoprecipitated by anti-VEGFR2 or anti-FLAG antibodies and was detected with anti-nephrin or anti-Myc antibodies (Fig. 2*C*); reciprocal experiments verified the findings. No interaction was found in cells lysate incubated with control IgG. In addition, VEGFR2-nephrin interaction was further confirmed using an independent method, mass spectrometry. COS-7 cells were transfected with full-length VEGFR2 and nephrin and immunoprecipitated with anti-nephrin antibody, and the eluate was resolved by SDS-PAGE. Bands at ~180 kDa were excised and subjected to *in situ* enzymatic digestion followed by mass spectrometry analysis. Three peptides from the cytoplasmic domain of mouse VEGFR2 (TGYLSIVMDPDELPLDER, FGNLSTYLR, and GAFGQVIEADAFGIDK) were identified in the nephrin immunoprecipitate (Fig. 2*D*). Taken together, these findings demonstrate an interaction between VEGFR2 and nephrin in cultured podocytes and *in vitro*.

Nephrin Binds VEGFR2 Directly via Its Cytoplasmic Domain—Nephrin is a key component of a transmembrane protein complex at the podocyte plasma membrane, which plays structural and signaling roles (4, 5). Nephrin cytoplasmic domain has been shown to associate with several proteins, including Neph1 (36), podocin (39), CD2AP (40), and Nck (11, 14, 17), suggesting that nephrin participates in a number of intracellular signaling transduction pathways. To test whether the VEGFR2-nephrin interaction is direct and mediated through the CD of nephrin, purified nephrin cytoplasmic domain (GST-CD-nephrin) was incubated with purified Flag-VEGFR2 full-length *in vitro*, as described under "Experimental Procedures." The GST-binding assay showed that the cytoplasmic domain of nephrin binds VEGFR2 *in vitro*, indicating a direct interaction (Fig. 3*A*). The purity of the GST construct was confirmed by Coomassie Blue staining (Fig. 3*B*).

To further define whether this association is direct, we used overlay blot assays. Purified GST-CD-nephrin (2–10 μg) was resolved by SDS-PAGE and transferred to nitrocellulose membranes, and membranes were overlaid with purified FLAG-VEGFR2, followed by immunoblotting with anti-FLAG antibody. Full-length FLAG-VEGFR2 bound specifically to GST-CD-nephrin in a concentration-dependent manner, but not to GST-control (Fig. 3*C*). Together, these findings demonstrate that nephrin binds to VEGFR2 directly through its cytoplasmic domain.

Cytoplasmic Domains of VEGFR2 and Nephrin Interact—To evaluate which VEGFR2 domain interacts with nephrin, we generated a series of FLAG-tagged constructs encoding three protein domains as follows: the VEGFR2 cytoplasmic domain (CD-VEGFR2, 561 amino acids), its proximal fragment (VEGFR2-162, 162 amino acids), and its distal fragment (VEGFR2-399, 399 amino acids) (Fig. 4*A*). Each FLAG-tagged VEGFR2 fragment was transiently co-transfected with full-length nephrin into COS-7 cells and immunoprecipitated with anti-FLAG antibody. Nephrin co-immunoprecipitated with VEGFR2 cytoplasmic domain (CD-VEGFR2) and both of its fragments, VEGFR2-162 and VEGFR2-399 (Fig. 4*B*). Reverse co-IP experiments performed with anti-Myc antibody, followed by immunoblotting with anti-FLAG antibody confirmed nephrin association with both VEGFR2 cytoplasmic domains (Fig. 4*C*). Quantitation of immunoprecipitate/lysate ratios showed similar association, Fig. 4, *B* and *C*, $n = 3$). These data suggested that at least two sequences of VEGFR2 cytoplasmic domain interact with nephrin. GST-binding assays were performed to evaluate this possibility. Purified FLAG-VEGFR2-162 or VEGFR2-399 proteins were incubated with purified GST-CD-nephrin, resolved by SDS-PAGE, and examined by Western blotting. In agreement with the previous co-IP data, nephrin cytoplasmic domain associated with VEGFR2-162 and with VEGFR2-399 (Fig. 4*D*).

Nephrin Tyrosine Phosphorylation Modulates VEGFR2-Nephrin Interaction—Nephrin has nine tyrosine residues in its intracellular domains. Verma *et al.* (13) demonstrated that Fyn binds directly to the nephrin cytoplasmic domain via its SH2 domain and phosphorylates the cytoplasmic domain of nephrin both *in vitro* and *in vivo*. To assess whether VEGFR2-nephrin interaction requires tyrosine phosphorylation of nephrin cyto-

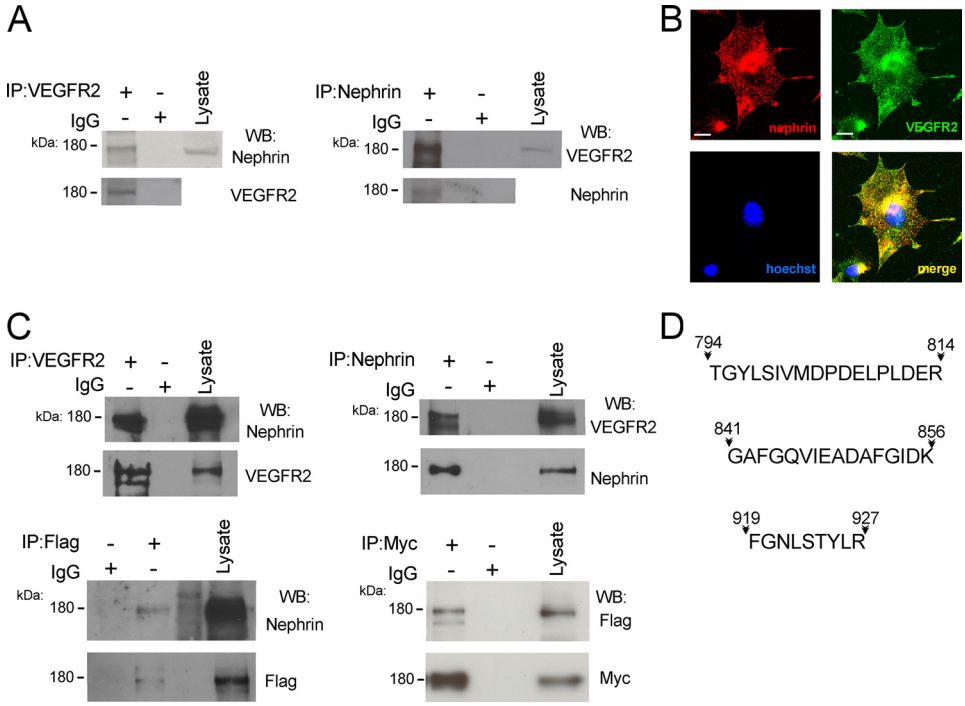

FIGURE 2. **Endogenous and transfected VEGFR2 and nephrin interact in culture cells.** *A*, endogenous nephrin-VEGFR2 co-IP from differentiated podocyte cell lysate. Anti-VEGFR2 and anti-nephrin antibodies were used, followed by WB with reciprocal antibody (upper blots); negative control is rabbit IgG, and inputs of each IP are shown (lower blots). *B*, immunolocalization of VEGFR2 (*green*) and nephrin (*red*) in differentiated podocytes. Nuclei were stained with Hoechst 33342 (*blue*), and merge image shows co-localization (*yellow*). *Scale bar*, 20 μm. *C*, nephrin-VEGFR2 co-IP from COS-7 cells transfected with full-length FLAG-VEGFR2 and Myc-tagged nephrin, using anti-VEGFR2, anti-FLAG, anti-nephrin, and anti-Myc antibodies (upper blots), inputs for each IP experiment (lower blots), no binding was found with control IgG. Co-IP and immunocytochemistry experiments showed that VEGFR2 and nephrin interact and co-localize *in vitro*. Experiments were repeated at least three times. *D*, COS-7 cells transfected with full-length VEGFR2, and nephrin were subjected to nephrin IP and resolved by SDS-PAGE. Bands at ~180 kDa were digested with trypsin, the resulting peptides were analyzed by LC-MS/MS. Peptides corresponding to amino acids 794–814, 841–856, and 919–927 of mouse VEGFR2 cytoplasmic domain were identified. kDa, molecular mass.

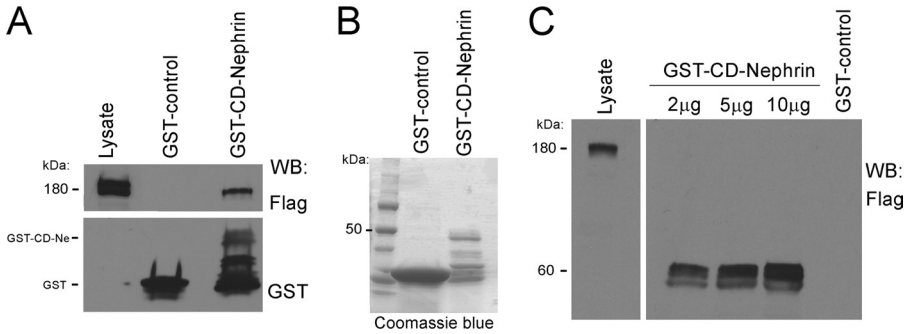

FIGURE 3. **Direct interaction between VEGFR2 and nephrin cytoplasmic domains.** *A*, GST-binding assay demonstrates direct association between VEGFR2 and cytoplasmic domain of nephrin. Purified recombinant GST-CD-nephrin was incubated *in vitro* with purified full-length FLAG-VEGFR2, resolved, and immunoblotted with anti-FLAG antibody. Positive control, lysate of COS-7 cells transfected with VEGFR2. *B*, representative Coomassie Blue gel of GST-control and GST-CD-nephrin in BL21 bacteria. *C*, overlay assay shows that nephrin binds VEGFR2 directly through its cytoplasmic domain. Increasing amount of purified GST-CD-nephrin (*Ne*) was resolved, probed with purified FLAG-VEGFR2, and immunoblotted with anti-FLAG antibody. Positive control is as described in *A*.

plasmic domain, purified full-length FLAG-VEGFR2 was incubated with purified GST-CD-nephrin expressed in BL21 or TKB1 *E. coli*. TKB1 harbor an inducible Elk receptor tyrosine kinase domain not contained in receptor tyrosine kinase-deficient BL21 *E. coli* (14). Upon transformation with the relevant plasmid, TKB1 produced GST-CD-nephrin phosphorylated on all of its tyrosine residues. Using this approach, VEGFR2 showed increased association with GST-CD-nephrin in a tyrosine phosphorylation-dependent manner (ratio TBK:BL21 = 1.8 ± 0.2, $p < 0.05$, $n = 4$) (Fig. 5*A*). When phosphorylated purified GST-CD-nephrin was incubated with the purified FLAG-VEGFR2 cytoplasmic domain proximal 162 amino acids and terminal 399 amino acids, CD-nephrin/VEGFR2-162 interaction did not change (TBK:BL21 = 1 ± 0.03, p = nonsignificant, $n = 3$) (Fig. 5*B*), whereas the interaction between phosphorylated CD-nephrin and VEGFR2-399 increased significantly (ratio TBK:BL21 = 3 ± 0.5, $p < 0.05$, $n = 3$, Fig. 5*C*).

To determine which phosphorylated tyrosine site(s) from the cytoplasmic domain of nephrin modulate the VEGFR2-nephrin interaction, full-length purified FLAG-VEGFR2 was incubated with purified recombinant GST-CD-nephrin or GST-CD-nephrin mutated in one, two, or both YD*X*V motifs, replacing tyrosine for phenylalanine to mimic unphosphorylated tyrosine, expressed in TKB1 (Fig. 5*D*). We observed that the asso-

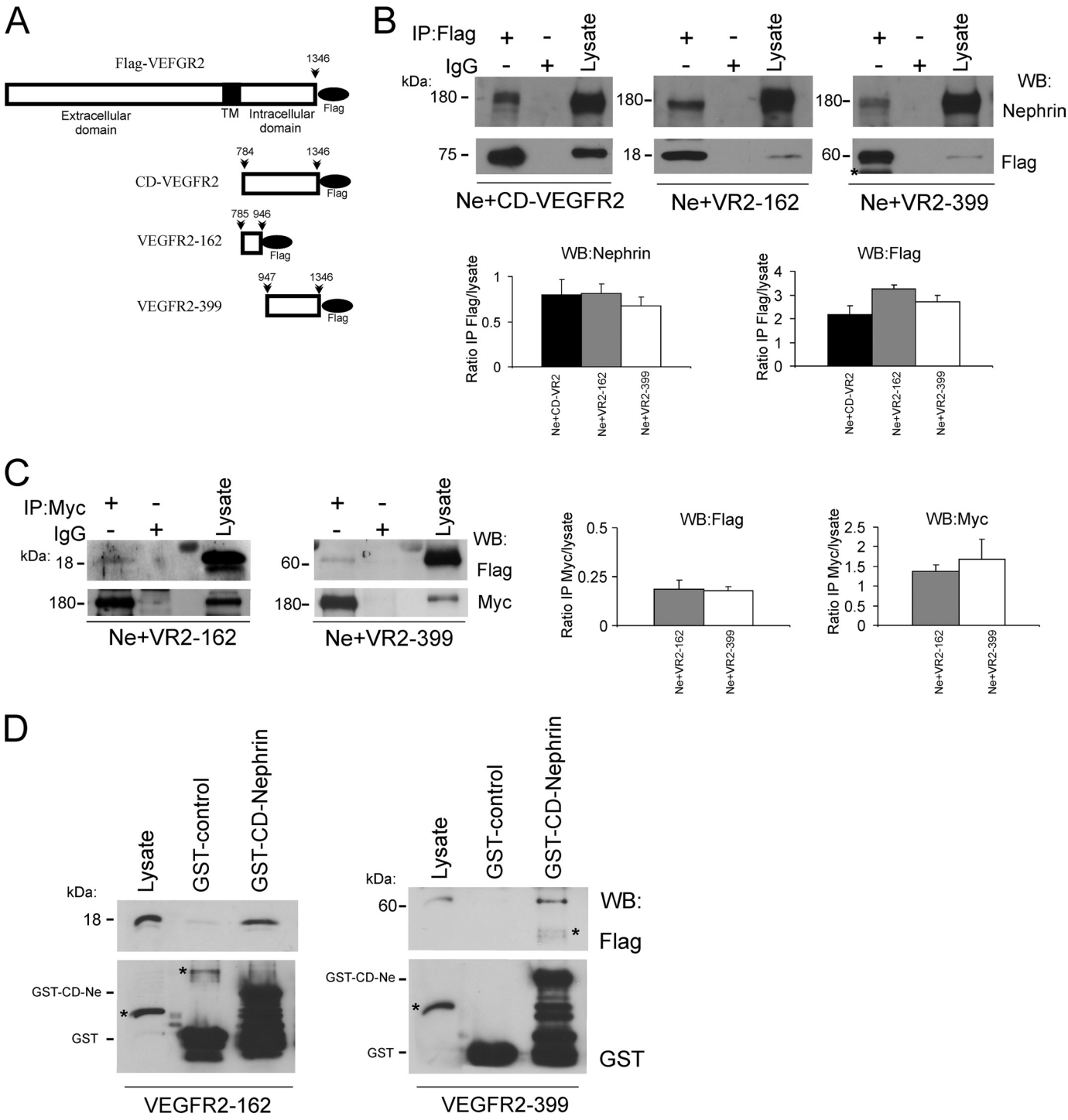

FIGURE 4. **Nephrin-binding regions are identified in VEGFR2 cytoplasmic domain.** *A*, scheme of VEGFR2 constructs. Full-length VEGFR2, VEGFR2 cytoplasmic domain (CD-VEGFR2), VR2-162 encoding the first 162 amino acids, and VR2-339 encoding the terminal 399 amino acids of the CD-VEGFR2, are all tagged with the C-terminal FLAG epitope. The *black bar* indicates the transmembrane domain. *B* and *C*, COS-7 cells were transfected with CD-VEGFR2, VR2-162, or VR2-399 and full-length nephrin (*Ne*), immunoprecipitated with anti-FLAG or anti-Myc antibodies, and immunoblotted with anti-nephrin or anti-FLAG antibodies, respectively. Nephrin binds CD-VEGFR2. Two independent nephrin-binding regions are identified in VEGFR2 by co-IP with VR2-162 or VR2-399 constructs. The results of three independent experiments were quantified by densitometry and depicted as IP:lysate ratios. *D*, purified GST-CD-nephrin was incubated *in vitro* with purified VR2-162 or VR2-399, eluates were resolved and immunoblotted with anti-FLAG antibody. Representative immunoblot demonstrates CD-nephrin direct interaction with two independent regions of CD-VEGFR2. All experiments were repeated at least three times. kDa indicates molecular mass. An *asterisk* indicates nonspecific bands.

ciation between VEGFR2 and CD-nephrin was increased in Y1191F mutant (Y1191F:CD-nephrin 1.7 ± 0.02, $p < 0.05$, $n = 4$) and decreased in Y1208F mutant (Y1208F:CD-nephrin 0.4 ± 0.1; $p < 0.05$, $n = 4$) (Fig. 5, *E* and *F*). These data suggest that Tyr-1191 and Tyr-1208 are involved in VEGFR2-nephrin interaction and that although Tyr-1208 phosphorylation increases nephrin-VEGFR2 interaction, Tyr-1191 phosphorylation does the opposite. The purity of GST-CD-nephrin

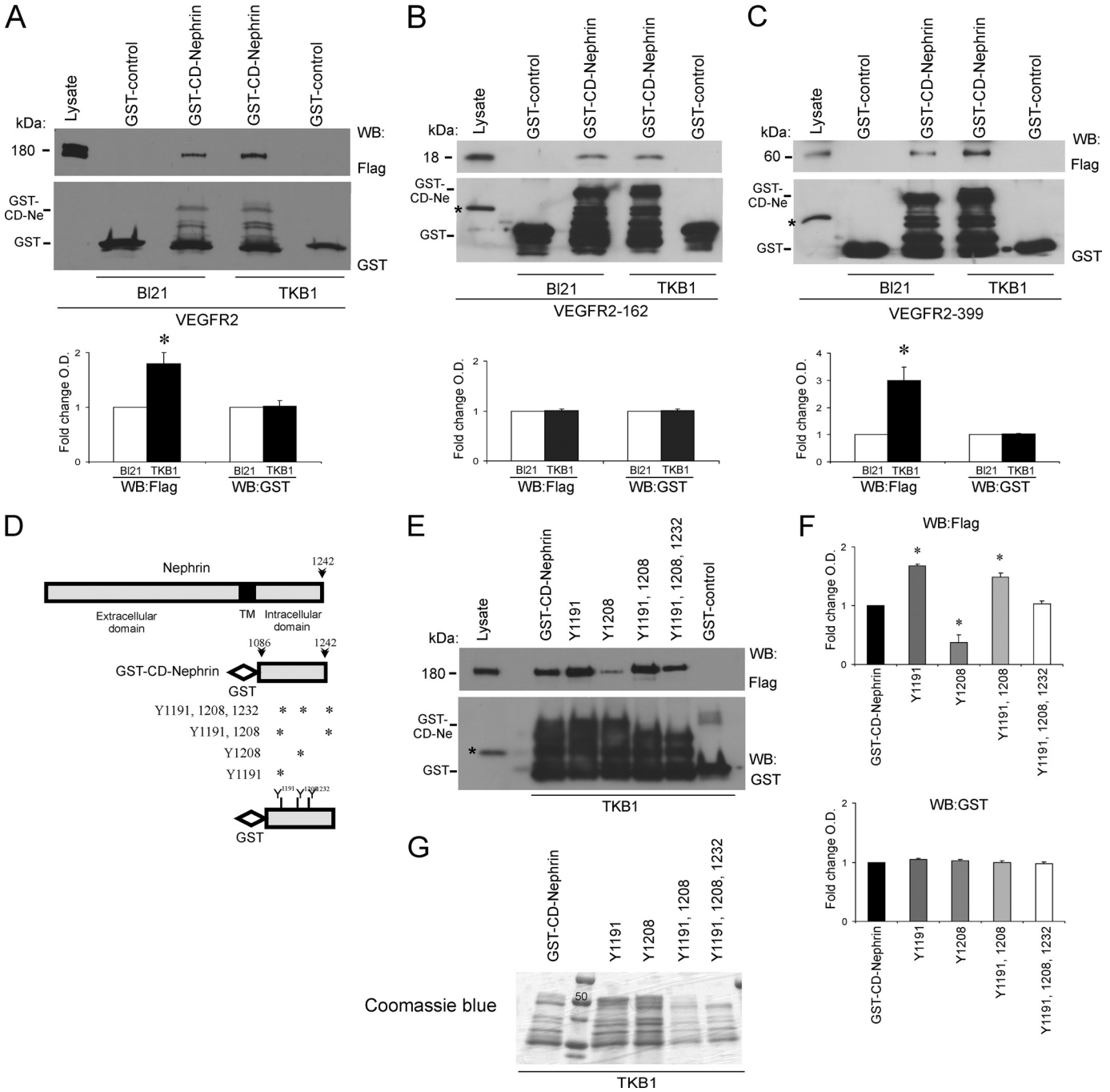

FIGURE 5. **VEGFR2-nephrin interaction is modulated by tyrosine phosphorylation of nephrin cytoplasmic domain.** *A*, *in vitro* GST-binding assays with purified GST-CD-nephrin incubated with purified full-length FLAG-VEGFR2. Tyrosine phosphorylation of CD-nephrin (*Ne*; *TKB1*) increases the direct interaction with VEGFR2, as compared with non-phosphorylated CD-nephrin (BL21). *B* and *C*, GST-binding assay shows that nephrin tyrosine phosphorylation (*TKB1*) enhances the interaction with VEGFR2-399, whereas it does not alter the interaction with VEGFR2-162. GST alone was used as negative control. Bar graphs show quantification of densitometric analysis of four independent experiments; data were normalized for BL21 and expressed as mean ± S.E. *, $p < 0.05$. *D*, schemes depict full-length nephrin, the predicted transmembrane domain (*TM*), GST-CD-nephrin, and mutation analysis of CD-nephrin tyrosine residues; *asterisks* indicate the residue(s) substituted by phenylalanine in each of the four constructs. *E*, GST binding assays showed that the association between purified VEGFR2 and phosphorylated CD-nephrin decreased when Tyr-1208 was mutated, and increased when Tyr-1191 was mutated. *F*, quantitation of densitometric analysis of three independent experiments, normalized for GST-CD-nephrin and expressed as mean ± S.E. An *asterisk* indicates $p < 0.05$. *G*, representative Coomassie Blue gel of GST-CD-nephrin and mutants in TKB1 bacteria.

and mutants in TKB1 bacteria are shown by Coomassie Blue gel (Fig. 5*G*).

Tyrosine Phosphorylation of VEGFR2 Decreases Interaction with Nephrin—To examine whether autophosphorylation of VEGFR2 upon ligand binding modulates its interaction with nephrin, COS-7 cells were transiently transfected both with full-length FLAG-VEGFR2 and nephrin and were then exposed to recombinant $VEGF_{165}$ ($rVEGF_{165}$) in the presence of heparin, which enhances VEGF-induced VEGFR2 activation (41). When COS-7 lysate was immunoprecipitated with anti-VEGFR2 antibody, nephrin co-immunoprecipitated with VEGFR2, both in the presence and in the absence of $rVEGF_{165}$.

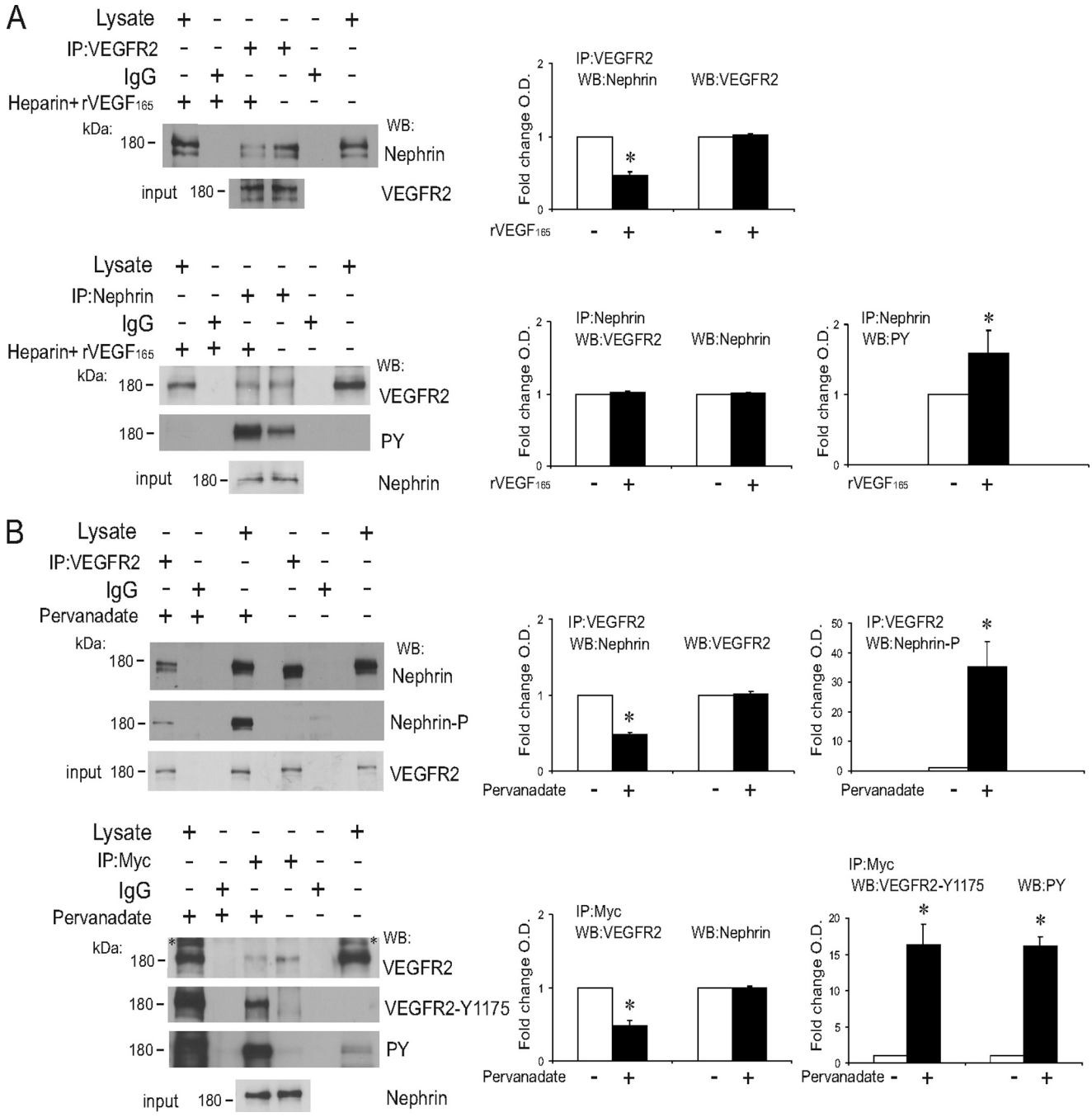

FIGURE 6. **Tyrosine phosphorylation decreases nephrin-VEGFR2 interaction.** *A*, COS-7 cells transfected with full-length VEGFR2 and nephrin were stimulated with heparin (50 units/ml) or heparin+rVEGF$_{165}$ (50 ng/ml) for 30 min. rVEGF$_{165}$ induced VEGFR2 phosphorylation and decreased nephrin-VEGFR2 association. IP of anti-VEGFR2 or anti-nephrin antibodies are shown as indicated. WB of anti-nephrin, anti-VEGFR2, or anti-phosphotyrosine (*PY*) antibodies are shown as indicated. Inputs of each IP experiment are shown (lower gels). *B*, tyrosine phosphorylation of both nephrin and VEGFR2 decreases their interaction in COS-7 cells transfected with full-length VEGFR2 and nephrin, treated with tyrosine phosphatase inhibitor pervanadate (50 μM) or vehicle for 30 min. IP of anti-VEGFR2 or anti-Myc antibodies are shown as indicated. WB of anti-nephrin, anti-phospho-nephrin (nephrin-P), anti-VEGFR2, anti-VEGFR2$^{Tyr\text{-}1175}$, and anti-phosphotyrosine (*PY*) antibodies are shown as indicated. Inputs for each IP experiment are shown (lower gels). Bar graphs show quantification of densitometric analysis of four independent experiments, normalized to control, expressed as mean ± S.E. An *asterisk* indicates $p < 0.05$. kDa indicates molecular mass. An *asterisk* indicates nonspecific bands in immunoblots.

Interestingly, we found that the quantity of VEGFR2-bound nephrin was reduced when cells had been exposed to the ligand (IP rVEGF$_{165}$:control = 0.46 ± 0.05, $p < 0.05$, $n = 8$; Fig. 6*A*). Because co-IP experiments showed that VEGFR2/CD-nephrin interaction is increased when CD-nephrin is tyrosine-phosphorylated and decreased when VEGFR2 is tyrosine phosphorylated, we next asked whether VEGFR2-nephrin interaction was altered when both proteins were phosphorylated. COS-7 cells transiently transfected with full-length VEGFR2 and nephrin were exposed to pervanadate, a tyrosine phosphatase inhibitor, for 30 min. Immunoprecipitation experiments with anti-VEGFR2 or anti-nephrin/Myc antibodies were performed. Notably, in the presence of pervanadate, the amount of co-immunoprecipitated nephrin, and VEGFR2 was decreased

(pervanadate:control = 0.48 ± 0.07, $p < 0.05$, $n = 5$; and 0.47 ± 0.03, $p < 0.05$, $n = 6$; Fig. 6*B*). This result is consistent with the finding that the Tyr-1191 residue is inhibitory. In the absence of pervanadate, we observed that VEGFR2 has baseline phosphorylation, but nephrin phosphorylation was not detected (Fig. 6*B*). Together, these results suggest that VEGFR2-nephrin interaction is not fully phosphorylation-dependent but is modulated by tyrosine phosphorylation such that VEGFR2 tyrosine phosphorylation decreases the association with nephrin.

VEGFR2-Nephrin and Nck Form a Signaling Complex That Binds Actin—Several groups demonstrated that upon nephrin phosphorylation on Tyr-1191, Tyr-1208, and Tyr-1232, the cytoplasmic domain of nephrin interacts with Nck, inducing the assembly of actin filaments (17, 36). VEGFR2 cytoplasmic domain interaction with Nck was shown to depend on Tyr-1214-VEGFR2 phosphorylation, triggering actin polymerization and stress fiber formation (24). To determine whether Nck is part of a signaling complex with VEGFR2-nephrin, COS-7 cells were transfected with full-length Nck, nephrin, and VEGFR2. Cell lysates were immunoprecipitated with anti-Nck antibody, followed by Western blot with anti-nephrin or anti-VEGFR2 antibodies. As shown in Fig. 7*A*, Nck associates with both nephrin and VEGFR2, and co-immunoprecipitation of the three proteins can be attained with antibodies to each. Moreover, we observed that these three endogenous proteins assemble as a complex also in cultured podocytes (Fig. 7*B*). Furthermore, the VEGFR2-nephrin-Nck complex appeared to engage endogenous α-actin, both in transfected COS-7 cells and in podocytes (Fig. 7, *A* and *B*).

When COS-7 cells were transfected with nephrin and VEGFR2-162 or VEGFR2-399 constructs, endogenous Nck and α-actin immunoprecipitated with Myc-nephrin and with both FLAG-VEGFR2 fragments (Fig. 7*C*). We also observed that Nck and α-actin co-immunoprecipitated with anti-FLAG antibody in COS-7 cells transfected only with VEGFR2-399 construct (Fig. 7*D*). In contrast, in COS-7 cells transfected only with VEGFR2-162, α-actin co-immunoprecipitated with VEGFR2-162, but Nck did not (Fig. 7*D*). Together, these data imply that endogenous Nck associates with nephrin and also interacts with the terminal portion of the cytosolic domain of VEGFR2 (VEGFR2-399) to form a complex. In this setting, α-actin associates with nephrin and with VEGFR2 cytosolic domains, whereas α-actin interaction with VEGFR2-162 appears to be independent of Nck.

VEGFR2-Nephrin Interaction Transduces Extracellular VEGF-A Signals to Actin Cytoskeleton—To examine the functional significance of VEGFR2-nephrin interaction at the cellular level, we examined the effect of VEGF-A on cell shape. COS-7 cells transfected with Myc-nephrin, FLAG-VEGFR2, or with both constructs were serum-starved, exposed to 50 ng/ml $rVEGF_{165}$ or vehicle for 30 min, fixed, stained with rhodamine phalloidin, and examined by confocal microscopy (Fig. 8, *A–F*). $VEGF_{165}$-induced changes in the shape of cells expressing VEGFR2 and nephrin, whereas cells exposed to vehicle or expressing nephrin or VEGFR2 only remained unaltered (Fig. 8, *A–D*). Morphometric analysis revealed that $VEGF_{165}$ induced a significant decrease in cell area in COS-7 cells expressing VEGFR2 and a more pronounced cell size reduction in those expressing nephrin + VEGFR2 (Fig. 8, *G* and *H*). These data suggest that in cells expressing nephrin and VEGFR2, VEGF-A extracellular signals modulate cell shape via VEGFR2-nephrin.

DISCUSSION

VEGF-A signals mediated by VEGFR2 are essential for the integrity of the glomerular filtration barrier. Although excessive VEGF-A causes podocyte effacement and proteinuria leading to kidney damage, the autocrine molecular mechanism mediating VEGF-induced podocyte effacement has not been defined. Nephrin signaling plays a central role in controlling podocyte slit diaphragm structure and function. Thus, gene defects in this pathway lead to disease, but the extracellular cues that modulate this pathway remain elusive. We showed previously that VEGFR2-nephrin association links VEGF and nephrin signaling pathways *in vivo* (25). In the present study, we explored how VEGFR2 and nephrin interact, and whether the VEGFR2-nephrin complex regulates podocyte shape.

This study demonstrates a direct interaction between VEGFR2 and nephrin in cultured cells and *in vitro*. Nephrin-VEGFR2 interaction was identified by co-immunoprecipitation in podocytes and in COS-7 cells transfected with the corresponding plasmids and was confirmed by mass spectrometry. VEGFR2 direct interaction with the nephrin cytoplasmic domain was demonstrated by GST-binding assay and confirmed by overlay assay. Because nephrin expression in the kidney is restricted to podocytes, these data strongly implicate a role for VEGFR2 signaling in this cell type. One report failed to detect VEGFR2 in podocytes and a glomerular phenotype in VEGFR2 floxed mice carrying nephrin-Cre (43), but Cre expression in podocytes was not quantitated to assess whether VEGFR2 ablation was complete. The lack of phenotype may be due to partial VEGFR2 knockdown, given that VEGFR2 heterozygotes are normal (20). Our group and others detected podocyte VEGFR2 expression *in vivo* by immunoelectron microscopy and co-immunoprecipitation (25, 26). Collectively, our data identify VEGFR2 as a novel component of the slit diaphragm signaling complex and further support our previous studies indicating that VEGF-A signaling plays a cell autonomous role in the control of podocyte shape and function (25).

Nephrin intracellular domain interacts with several proteins, including Neph1, podocin, CD2AP, p85, the regulatory subunit of PI3K, Nck, β-arrestin-2, and PKCα. These interactions scaffold and mediate nephrin signaling to the actin cytoskeleton and regulate podocyte survival, endocytosis, and metabolism (12, 39, 40, 44–46). Here, we show that VEGFR2-nephrin interaction occurs in the presence or absence of tyrosine phosphorylation of both proteins. However, VEGF stimulation and nephrin phosphorylation decrease VEGFR2-nephrin interaction in intact cells. Phosphorylation of the YD*X*V motifs of nephrin intracellular domain by Fyn enables the recruitment of adaptor protein Nck and enhances nephrin association with other slit diaphragm proteins (14, 16, 17). Similarly, VEGFR2 Tyr-1214 autophosphorylation triggers the recruitment and phosphorylation of Nck and Fyn (24), which form a complex, leading to actin polymerization, stress fiber formation, and endothelial cell migration (24, 47). We found that Nck associates with both nephrin and VEGFR2 in podocytes and transfected cells. Previ-

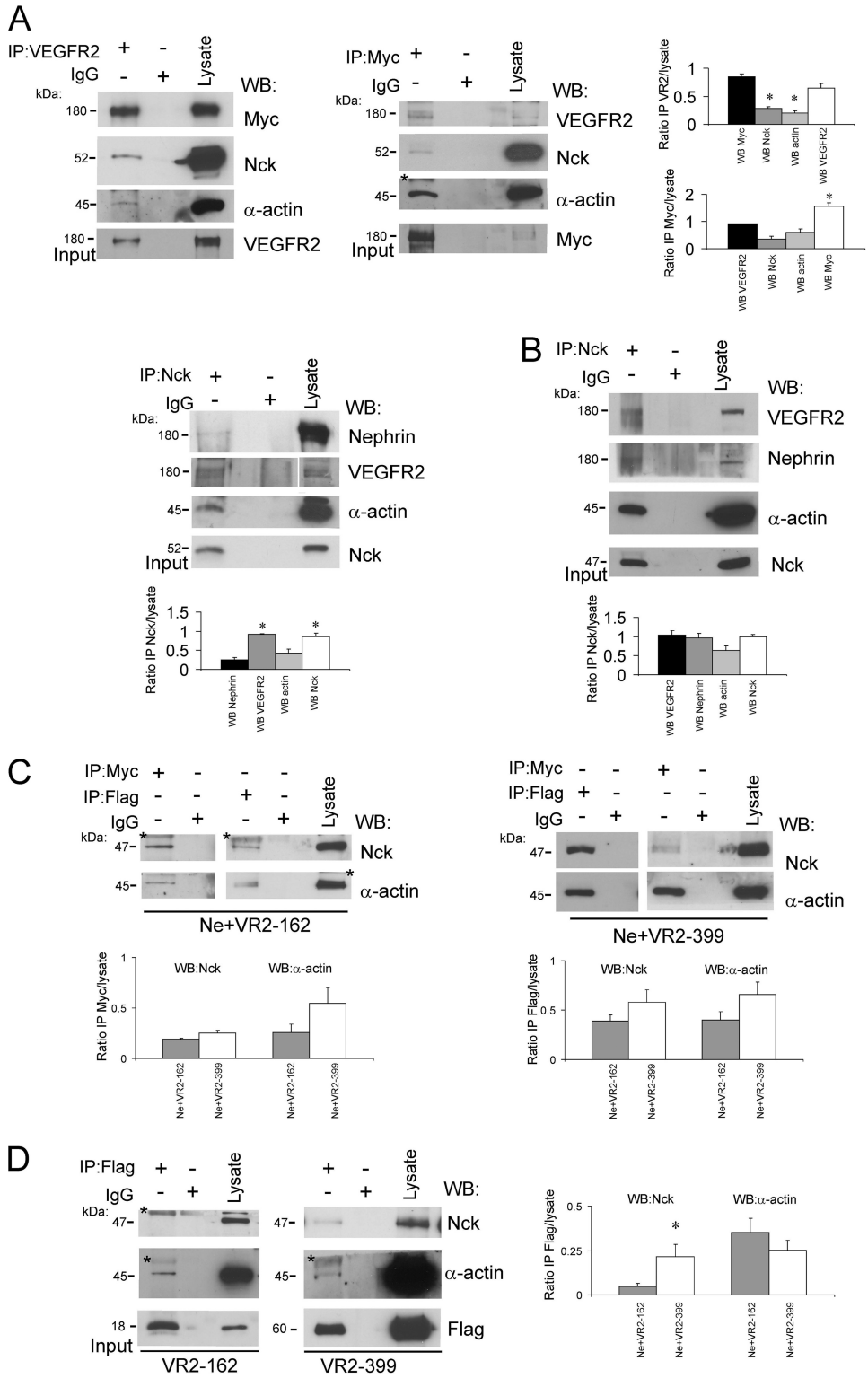

FIGURE 7. **Nck and α-actin interact with the VEGFR2-nephrin complex.** *A*, Nck and α-actin associate with the VEGFR2-nephrin complex in COS-7 cells transfected with FLAG-Nck (52 kDa), full-length VEGFR2, and nephrin. IP of anti-Nck, anti-VEGFR2, or anti-nephrin antibodies were performed as indicated. WB of anti-nephrin, anti-Myc, anti-VEGFR2, anti-Nck, and anti-α-actin antibodies were performed as indicated. *B*, endogenous Nck (47 kDa) and actin interact with endogenous VEGFR2 and nephrin in cultured podocytes. IP of anti-Nck, anti-VEGFR2, or anti-nephrin were performed as indicated. WB of anti-nephrin, anti-VEGFR2, anti-Nck, and anti-α-actin antibodies were performed as indicated. Inputs of each IP are shown (lower gels). *C*, endogenous Nck and actin associate with transfected nephrin and VEGFR2-CD fragments VR2-162 and VR2-399 in COS-7 cells. IP of anti-Myc and anti-FLAG antibodies were performed as indicated. WB of anti-Nck or anti-actin antibodies were performed as indicated. *D*, endogenous Nck interacts with VEGFR2 C-terminal fragment (VR2-399), and does not interact with VR2-162, whereas both VEGFR2 fragments associate with actin in COS-7 cells transfected with VR2-162 or VR2–339, suggesting that VR2-162-actin interaction is Nck-independent. IP of anti-FLAG antibody is shown. WB of anti-Nck or anti-actin antibodies were performed as indicated. Inputs of each IP are shown (lower gels). The results of three or more independent experiments were quantified by densitometry and depicted as IP:lysate ratios. kDa indicates molecular mass. An *asterisk* indicates nonspecific bands.

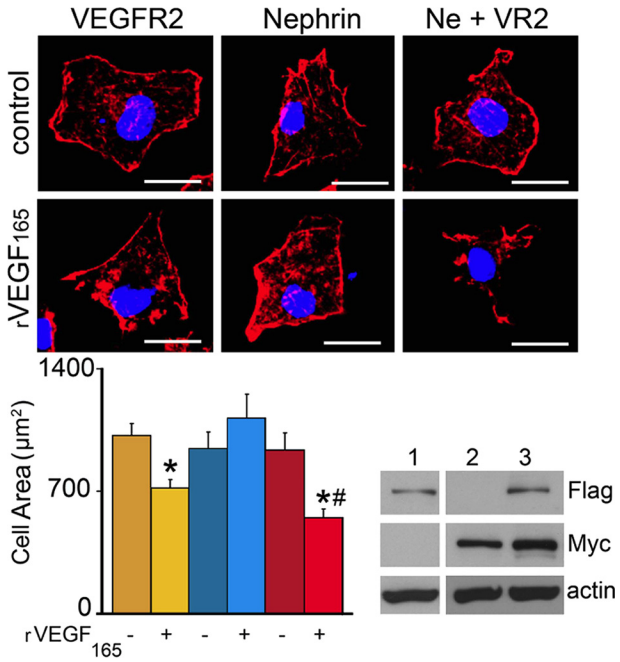

FIGURE 8. **VEGF-A signaling via VEGFR2-nephrin induces cell shape change.** *A*, COS-7 cells transfected with FLAG-VEGFR2, Myc-nephrin, or both constructs (*Ne+VR2*) were exposed to vehicle or $rVEGF_{165}$ for 30 min, fixed, and stained with rhodamine-phalloidin. $VEGF_{165}$ induced cell shape change only in expressing nephrin+VEGFR2 cells. *B*, morphometric analysis of cell area showed a decrease in cell size in VEGFR2-expressing cells (*yellow bar*), and a more pronounced decrease in cell size in nephrin+VEGFR2-expressing cells (*red bar*). Cell area (μm^2) expressed as mean ± S.E., 15 + 2.4 cells/experimental condition. *Asterisks* indicate $p < 0.05$ *versus* vehicle; #, $p < 0.05$ Ne+VR2 *versus* VEGFR2 alone. C, FLAG and Myc WB from COS-7 cells transfected with VEGFR2 (*lane 1*), nephrin (*lane 2*), and nephrin+VEGFR2 (*lane 3*), actin is shown as loading control.

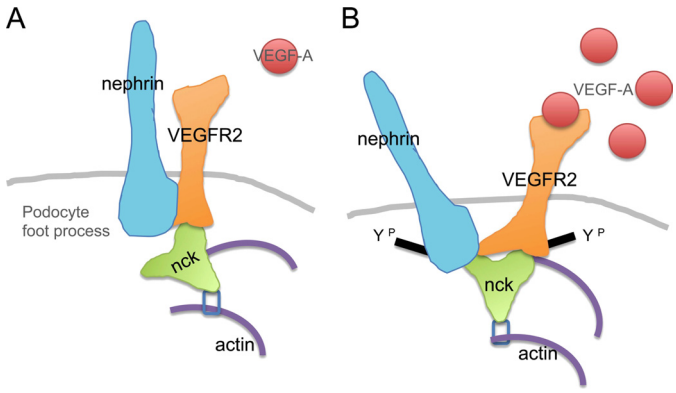

FIGURE 9. **Model of VEGFR2-nephrin interaction in podocytes.** *A*, in control conditions, VEGFR2 interacts directly with nephrin and forms a complex with Nck and actin. *B*, upon VEGF-A binding, nephrin-VEGFR2 interaction decreases and induces changes in shape and size in cultured cells.

ous reports demonstrated a direct interaction between Nck and nephrin (14). We confirmed that Nck binds to the VEGFR2 cytoplasmic domain that includes only Tyr-1214 (24). In addition, our data suggest that VEGFR2 cytoplasmic domain and Nck bind nephrin independently. Together, these findings indicate that VEGFR2, nephrin and Nck form a multiprotein complex in podocytes, which is modulated by VEGF-induced phosphorylation.

The actin cytoskeleton plays an essential role in the maintenance of podocyte shape and function. Several proteins that interact with nephrin intracellular domain are involved in the regulation of the actin cytoskeleton, including Nck and CD2AP (3, 13, 15). Nck SH3 domains bind neuronal when nephrin is phosphorylated by Fyn (13, 15). Neuronal Wiskott-Aldrich syndrome protein activates the Arp2/3 complex and regulates podocyte actin dynamics (15, 16, 48). We determined that actin is a component of the VEGFR2-nephrin-Nck complex, linking VEGF-A signals to the podocyte cytoskeleton. Moreover, we showed that VEGF-A signaling via VEGFR2-nephrin complex induces changes in cell shape, resulting in decreased cell area (Fig. 8). Consistent with these findings, VEGF-A signaling induces changes in endothelial cell morphology *in vitro* and *in vivo* (49, 50). Podocytes generate contractile forces via non-muscle myosins, α-actinin-4, and actin interaction, which are thought to allow shape adjustments in response to dynamic glomerular capillary pressure changes (3, 51). Mutations in these proteins in mice and humans also result in podocyte effacement (52). VEGF-induced cell shape change involving nephrin-VEGFR2 is reminiscent of VEGF-induced foot process effacement observed previously *in vivo* (25, 31). Collectively, our findings provide a molecular mechanism for the observation that induction of podocyte $VEGF_{164}$ overexpression in mice increases podocyte VEGFR2 phosphorylation and down-regulates nephrin, causing podocyte foot process effacement and proteinuria (25, 31). Moreover, increased VEGF-A, podocyte effacement and nephrin down-regulation have been demonstrated in mice and humans with diabetic nephropathy by our group and others (29, 30).

The mechanism of VEGF-induced nephrin down-regulation has not been defined. Upon VEGF-A binding, VEGFR2 autophosphorylation at Tyr-1175 mediates PLCγ binding, leading to PKC activation (19, 21, 22). Interestingly, PKCα mediates the effect of hyperglycemia on nephrin-β-arrestin2 interaction, increasing nephrin endocytosis in podocytes (45, 46). PKCα negatively regulates VEGF signaling and endothelial nitric oxide synthase phosphorylation in endothelial cells (53). Together, these findings raise the possibility that VEGFR2 signaling may play an important role in the regulation of nephrin endocytosis via PKCα.

In summary, the present studies demonstrate a direct interaction between the slit diaphragm protein nephrin and VEGFR2, the signaling receptor for VEGF-A. We show that the VEGFR2-nephrin interaction is modulated by tyrosine phosphorylation and that the VEGR2-nephrin complex involves Nck and actin. Moreover, VEGF-A signaling via this complex results in decreased cell size. These findings identify a novel signaling pathway that links extracellular VEGF-A signals directly to the slit diaphragm and to the podocyte actin cytoskeleton (Fig. 9). We propose that this pathway is necessary to maintain the dynamic functional integrity of the slit diaphragm and plays a key role in the molecular mechanism of podocyte foot process effacement.

Acknowledgments—We thank L. Pattarini (ICGEB, Trieste, Italy) for the FLAG-VEGFR2 construct, C. Faul (University of Miami) and D. Alfandari (University of Massachusetts) for help with construct purification, and A. M. Salicioni and P. Visconti (University of Massachusetts) for critical review of the manuscript.

REFERENCES

1. Rodewald, R., and Karnovsky, M. J. (1974) *J. Cell Biol.* **60,** 423–433
2. Pavenstädt, H., Kriz, W., and Kretzler, M. (2003) *Physiol. Rev.* **83,** 253–307
3. Faul, C., Asanuma, K., Yanagida-Asanuma, E., Kim, K., and Mundel, P. (2007) *Trends Cell Biol.* **17,** 428–437
4. Ruotsalainen, V., Ljungberg, P., Wartiovaara, J., Lenkkeri, U., Kestila, M., Jalanko, H., Holmberg, C., and Tryggvason, K. (1999) *Proc. Natl. Acad. Sci. U.S.A.* **6,** 7962–7967
5. Tryggvason, K. (1999) *J. Am. Soc. Nephrol.* **10,** 2440–2445
6. Kestilä, M., Lenkkeri, U., Männikkö, M., Lamerdin, J., McCready, P., Putaala, H., Ruotsalainen, V., Morita, T., Nissinen, M., Herva, R., Kashtan, C. E., Peltonen, L., Holmberg, C., Olsen, A., and Tryggvason, K. (1998) *Mol. Cell* **1,** 575–582
7. Kaukinen, A., Kuusniemi, A. M., Lautenschlager, I., and Jalanko, H. (2008) *Nephrol. Dial. Transplant.* **23,** 1224–1232
8. Uchida, K., Suzuki, K., Iwamoto, M., Kawachi, H., Ohno, M., Horita, S., and Nitta, K. (2008) *Kidney Int.* **73,** 926–932
9. Wernerson, A., Dunér, F., Pettersson, E., Widholm, S. M., Berg, U., Ruotsalainen, V., Tryggvason, K., Hultenby, K., and Söderberg, M. (2003) *Nephrol. Dial. Transplant.* **18,** 70–76
10. Putaala, H., Sainio, K., Sariola, H., and Tryggvason, K. (2000) *J. Am. Soc. Nephrol.* **11,** 991–1001
11. Tryggvason, K., Pikkarainen, T., and Patrakka, J. (2006) *Cell* **125,** 221–224
12. Huber, T. B., Hartleben, B., Kim, J., Schmidts, M., Schermer, B., Keil, A., Egger, L., Lecha, R. L., Borner, C., Pavenstädt, H., Shaw, A. S., Walz, G., and Benzing, T. (2003) *Mol. Cell Biol.* **23,** 4917–4928
13. Verma, R., Wharram, B., Kovari, I., Kunkel, R., Nihalani, D., Wary, K. K., Wiggins, R. C., Killen, P., and Holzman, L. B. (2003) *J. Biol. Chem.* **278,** 20716–20723
14. Verma, R., Kovari, I., Soofi, A., Nihalani, D., Patrie, K., and Holzman, L. B. (2006) *J. Clin. Invest.* **116,** 1346–1359
15. Rohatgi, R., Nollau, P., Ho, H. Y., Kirschner, M. W., and Mayer, B. J. (2001) *J. Biol. Chem.* **276,** 26448–26452
16. Jones, N., Blasutig, I. M., Eremina, V., Ruston, J. M., Bladt, F., Li, H., Huang, H., Larose, L., Li, S. S., Takano, T., Quaggin, S. E., and Pawson, T. (2006) *Nature* **444,** 818–823
17. Jones, N., New, L. A., Fortino, M. A., Eremina, V., Ruston, J., Blasutig, I. M., Aoudjit, L., Zou, Y., Liu, X., Yu, G. L., Takano, T., Quaggin, S. E., and Pawson, T. (2009) *J. Am. Soc. Nephrol.* **20,** 1533–1543
18. Simon, M., Gröne, H. J., Jöhren, O., Kullmer, J., Plate, K. H., Risau, W., and Fuchs, E. (1995) *Am. J. Physiol.* **268,** F240–250
19. Neufeld, G., Cohen, T., Gengrinovitch, S., and Poltorak, Z. (1999) *FASEB J.* **13,** 9–22
20. Shalaby, F., Rossant, J., Yamaguchi, T. P., Gertsenstein, M., Wu, X. F., Breitman, M. L., and Schuh, A. C. (1995) *Nature* **376,** 62–66
21. Waltenberger, J., Claesson-Welsh, L., Siegbahn, A., Shibuya, M., and Heldin, C. H. (1994) *J. Biol. Chem.* **269,** 26988–26995
22. Takahashi, T., Yamaguchi, S., Chida, K., and Shibuya, M. (2001) *EMBO J.* **20,** 2768–2778
23. Sakurai, Y., Ohgimoto, K., Kataoka, Y., Yoshida, N., and Shibuya, M. (2005) *Proc. Natl. Acad. Sci. U.S.A.* **102,** 1076–1081
24. Lamalice, L., Houle, F., and Huot, J. (2006) *J. Biol. Cell* **281,** 34009–34020
25. Veron, D., Reidy, K. J., Bertuccio, C., Teichman, J., Villegas, G., Jimenez, J., Shen, W., Kopp, J. B., Thomas, D. B., and Tufro, A. (2010) *Kidney Int.* **77,** 989–999
26. Ku, C. H., White, K. E., Dei Cas, A., Hayward, A., Webster, Z., Bilous, R., Marshall, S., Viberti, G., and Gnudi, L. (2008) *Diabetes* **57,** 2824–2833
27. Guan, F., Villegas, G., Teichman, J., Mundel, P., and Tufro, A. (2006) *Am. J. Physiol.* **291,** F422–428
28. Foster, R. R., Saleem, M. A., Mathieson, P. W., Bates, D. O., and Harper, S. J. (2005) *Am. J. Physiol.* **288,** F48–57
29. Hovind, P., Tarnow, L., Oestergaard, P. B., and Parving, H. H. (2000) *Kidney Int.* **75,** S56–61
30. Veron, D., Bertuccio, C. A., Marlier, A., Reidy, K., Garcia, A. M., Jimenez, J., Velazquez, H., Kashgarian, M., Moeckel, G. W., and Tufro, A. (2011) *Diabetologia* **54,** 1227–1241
31. Veron, D., Reidy, K., Marlier, A., Bertuccio, C., Villegas, G., Jimenez, J., Kashgarian, M., and Tufro, A. (2010) *Am. J. Pathol.* **177,** 2225–2233
32. Holzman, L. B., St., John, P. L., Kovari, I. A., Verma, R., Holthofer, H., and Abrahamson, D. R. (1999) *Kidney Int.* **56,** 1481–1491
33. Mizuno, K., Tagawa, Y., Mitomo, K., Watanabe, N., Katagiri, T., Ogimoto, M., and Yakura, H. (2002) *J. Immunol.* **169,** 778–786
34. Jat, P. S., Noble, M. D., Ataliotis, P., Tanaka, Y., Yannoutsos, N., Larsen, L., and Kioussis, D. (1991) *Proc. Natl. Acad. Sci. U.S.A.* **88,** 5096–5100
35. Mundel, P., Reiser, J., Zuniga Mejia Borja, A., Pavenstadt, H., Davidson, G. R., Kriz, W., and Zeller, R. (1997). *Exp. Cell Res.* **236,** 248–258
36. Barletta G. M., Kovari I. A., Verma R. K., Kerjaschki D., and Holzman L. B. (2003) *J. Biol. Chem.* **278,** 19266–19271
37. Stone K. L., and Williams K. R. (2004). *Curr. Protoc. Protein Sci.*
38. Hirosawa, M., Hoshida, M., Ishikawa, M., and Toya, T. (1993) *Comput. Appl. Biosci.* **9,** 161–167
39. Huber, T. B., Kottgen, M., Schilling, B., Walz, G., and Benzing, T. (2001) *J. Biol. Chem.* **276,** 41543–41546
40. Shih, N. Y., Li, J., Cotran, R., Mundel, P., Miner, J. H., and Shaw, A. S. (2001) *Am. J. Pathol.* **159,** 2303–2308
41. Ashikari-Hada, S., Habuchi, H., Kariya, Y., and Kimata, K. (2005) *J. Biol. Chem.* **280,** 31508–31515
42. Shankland, S. J., Pippin, J. W., Reiser, J., and Mundel, P. (2007) *Kidney Int.* **72,** 26–36
43. Sison, K., Eremina, V., Baelde, H., Min, W., Hirashima, M., Fantus, I. G., and Quaggin, S. E. (2010) *J. Am. Soc. Nephrol.* **21,** 1691–1701
44. Lehtonen, S., Zhao, F., and Lehtonen, E. (2002) *Am. J. Physiol. Renal Physiol.* **283,** F734–743
45. Quack, I., Woznowski, M., Potthoff, S. A., Palmer, R., Königshausen, E., Sivritas, S., Schiffer, M., Stegbauer, J., Vonend, O., Rump, L. C., and Sellin, L. (2011) *J. Biol. Chem.* **286,** 12959–12970
46. Tossidou, I., Teng, B., Menne, J., Shushakova, N., Park, J. K., Becker, J. U., Modde, F., Leitges, M., Haller, H., and Schiffer, M. (2010) *PLoS One* **5,** e10185
47. Stoletov, K. V., Ratcliffe, K. E., Spring, S. C., and Terman, B. I. (2001) *J. Biol. Chem.* **276,** 22748–22755
48. Weaver, A. M., Young, M. E., Lee, W. L., and Cooper, J. A. (2003) *Curr. Opin. Cell Biol.* **15,** 23–30
49. Matsukawa, M., Sakamoto, H., Kawasuji, M., Furuyama, T, and Ogawa, M. (2009) *Genes Cells* **14,** 1167–1181
50. Strili, B., Kucera, T., Eglinger, J., Hughes, M. R., McNagny, K. M., Tsukita, S., Dejana, E., Ferrara, N., and Lammert, E. (2009) *Dev. Cell* **17,** 505–515
51. Saleem, M. A., Zavadil, J., Bailly, M., McGee, K., Witherden, I. R., Pavenstadt, H., Hsu, H., Sanday, J., Satchell, S. C., Lennon, R., Ni, L., Bottinger, E. P., Mundel, P., and Mathieson, P. W. (2008) *Am. J. Physiol. Renal Physiol.* **295,** F959–970
52. Mele, C., Iatropoulos, P., Donadelli, R., Calabria, A., Maranta, R., Cassis, P., Buelli, S., Tomasoni, S., Piras, R., Krendel, M., Bettoni, S., Morigi, M., Delledonne, M., Pecoraro, C., Abbate, I., Capobianchi, M. R., Hildebrandt, F., Otto, E., Schaefer, F., Macciardi, F., Ozaltin, F., Emre, S., Ibsirlioglu, T., Benigni, A., Remuzzi, G., and Noris, M. (2011) *N. Engl. J. Med.* **365,** 295–306
53. Rask-Madsen, C., and King, G. L. (2008) *Arterioscler. Thromb. Vasc. Biol.* **28,** 919–924